Controlled Amplification of DNA Brownian Motion Using Electrokinetic Noise

Shayan Lameh,[1] Lijie Ding,[1] and Derek Stein[1,*]

[1] *Department of Physics, Brown University, Providence, Rhode Island 02912, USA*

The application of voltage noise with the same statistical properties as fundamental thermal noise controllably amplified the Brownian motion of lambda DNA molecules suspended in solution inside a nanoslit. We analyzed the trajectories of single molecules and found that their self-diffusivity in the direction of the applied electric field increased in proportion with the variance of the voltage noise. The highest effective diffusivity achieved corresponded to an effective temperature of 5,300 K. However, unlike thermal noise, the voltage noise causes correlated fluctuations of different molecules and their segments. This technique unlocks a previously inaccessible effective temperature regime for studies and applications of noise-dependent phenomena.

INTRODUCTION

Noise plays a central role in chemical reactions [1], climate systems [2], gene regulation [3], and financial markets [4]. In micro and nanofluidic systems, thermal fluctuations are a fundamental form of noise. They give rise to the Brownian motion of suspended particles [5, 6], osmotic pressure [7], the elasticity of polymers [8], and depletion interactions between colloids [9, 10]. Fluidic devices provide a convenient arena to study exotic noise-driven phenomena, like giant acceleration of diffusion [11], stochastic resonance [12–14], and noise assisted barrier crossing [15, 16]. However, when we exclusively rely on thermal fluctuations as the source of noise, the freezing and boiling points of water severely restrict the range in which the noise level can be experimentally varied. Here we report a method to greatly raise the accessible noise level and amplify the Brownian motion of DNA molecules in nanoslits. We added an electrokinetic noise component with a noise level that we varied widely and independently of the temperature.

Figure 1 illustrates the experimental method. A nanoslit strongly confines DNA in the vertical dimension (z-direction) while allowing it to move freely across the relatively large slit width (x-direction) and along its length (y-direction). The motion of individual DNA molecules is tracked in the x and y dimensions using fluorescence optical microscopy. To influence the DNA dynamics, we impose a time-dependent voltage difference, $V(t)$, across the nanoslit using electrodes immersed in liquid reservoirs at either end. $V(t)$ has similar statistical properties to thermal fluctuations, but its amplitude can be adjusted. The resulting DNA dynamics correspond to a Brownian motion with amplified fluctuations along the length of the nanoslit. Our method operates in a manner reminiscent of the anti-Brownian electrophoretic (ABEL) trap [17], except that instead of cancelling the fluctuations of suspended objects, we use electrokinetic forces to amplify them.

It is convenient to characterize the lengthwise fluctuations of DNA in our setup by an effective temperature. "Noise temperature" commonly characterizes fluctuations in electronic circuits [18]; the motion of self-propelled swimmers can be characterized by an effective temperature [19]; and in a case of particular interest to us, temperature is used to parameterize the noise strength that gives rise to stochastic resonance [14, 20]. Our nanofluidic method enables us to impose an effective temperature that is adjustable and well above the boiling point of water. By tracking individual DNA molecules and analyzing their Brownian motions, we measured their equivalent temperatures in the lengthwise direction and found it could reach 5,300 K.

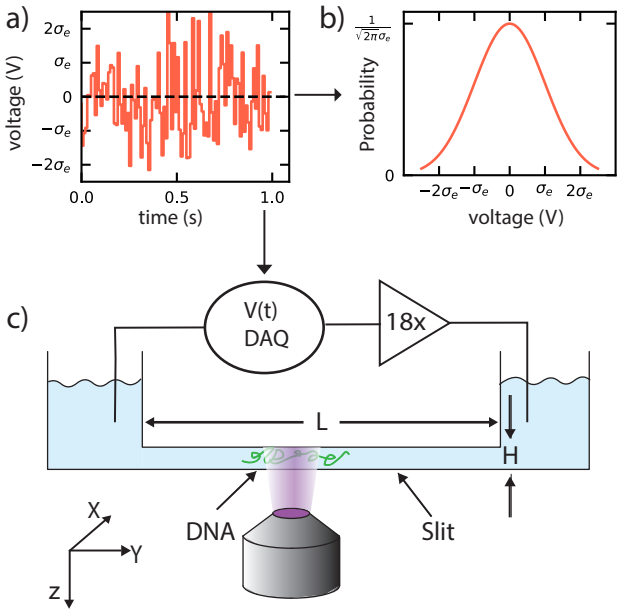

FIG. 1. Schematic of the method for electrokinetically amplifying Brownian motion. a) A typical trace of $V(t)$. b) Gaussian distribution of voltage fluctuations. c) Illustration of the nanoslit with a fluorescently stained DNA molecule and the optical microscopy system used to track the DNA motion. The sketch indicates L, H, and the orientation of the nanoslit relative to the coordinate system.

The Brownian motion of a DNA molecule is characterized by the growth of its mean square displacement

(MSD) in time,

$$\text{MSD} \equiv \left\langle (x_i(t+\Delta t) - x_i(t))^2 \right\rangle = 2D\Delta t, \quad (1)$$

where $x_i(t)$ is the generalized coordinate of molecule i, Δt is the time interval, $\langle ... \rangle$ denotes the ensemble average, and D is the self-diffusion constant, defined by [21]

$$D \equiv \int_0^\infty t \left\langle \dot{x}_i(t)\dot{x}_i(0) \right\rangle. \quad (2)$$

The Brownian motion is normally driven by thermal forces alone. In that case the overdamped Langevin equation describes the dynamics [22]

$$\dot{x}(t) = \frac{F(t)}{\zeta}, \quad (3)$$

where ζ is the viscous drag coefficient and $F(t)$ is a random thermal force with zero mean and zero autocorrelation, i.e. $\langle F(t) \rangle = 0$ and $\langle F(t)F(t') \rangle = 2\zeta k_B T \delta(t-t')$ [6], where k_B is the Boltzmann constant, T is the temperature, and $\delta(t)$ is the Dirac delta function. Combining Eqs. (2) and (3) gives D_0, the thermal self-diffusivity in one dimension

$$D_0 = \frac{k_B T}{\zeta}. \quad (4)$$

The application of $V(t)$ across the nanoslit generates an additional electrokinetic force in the y-direction, and the corresponding Langevin equation becomes

$$\dot{y}(t) = \frac{F(t)}{\zeta} + \mu \frac{V(t)}{L}, \quad (5)$$

where μ is the electrophoretic mobility of the DNA, and the ratio $V(t)/L$ gives the electric field inside the slit.

To mimic thermal noise using a signal generator with a finite bandwidth, we generate a band-limited Gaussian white noise signal for $V(t)$. This gives $\langle V(t) \rangle = 0$ and $\langle V(t)V(t') \rangle = \sigma_e^2 \left(\frac{\sin(2\pi B(t-t'))}{2\pi B(t-t')} \right)$[23, 24], where σ_e is the standard deviation and B is the bandwidth. When the bandwidth of the signal generator is large compared with that of the particle tracking system, we can approximate $\langle V(t)V(t') \rangle \approx \frac{\sigma_e^2}{2B}\delta(t-t')$. $V(t)$ and $F(t)$ have similar statistical properties, but they are not correlated with each other, so $\langle F(t)V(t') \rangle = 0$. From Eqs. (2) and (5), the self-diffusion constant in the y direction is

$$D_y = D_0 + \frac{1}{4B}\left(\frac{\mu\sigma_e}{L}\right)^2. \quad (6)$$

Equation 6 predicts that the minimum DNA diffusivity is given by the thermal value, D_0, and that voltage noise increases the diffusivity in the y direction by an amount proportional to the variance of $V(t)$. From Eqs. (4) and (6) we can define the effective temperature of Brownian motions in the y direction, T_{eff}, to be

$$T_{\text{eff}} = T\frac{D_y}{D_0}. \quad (7)$$

While $V(t)$ amplifies the fluctuations of a molecule's COM, it does not affect the relative fluctuations between different segments within a molecule or between the COMs of different molecules. A voltage applied across a nanofluidic slit establishes a uniform field within it, so every segment of every molecule inside it is subjected to the same electrokinetic force at a given moment. This difference between electrokinetic noise and thermal noise can be observed in the relative diffusion between two molecules.

Fluctuations in the separation between two molecules can be parameterized by a pairwise diffusion coefficient, D^p. We obtain D^p by applying Eq. (5) to a pair of DNA molecules subject to the same $V(t)$. This gives $\dot{y}_2(t) - \dot{y}_1(t) = \frac{1}{\zeta}(F_2(t) - F_1(t))$ for the y direction, where $F_2(t)$ and $F_1(t)$, are the forces of thermal noise on each DNA molecule. Combining $\langle F_1(t)F_2(t) \rangle = 0$ and Eq. (5) we obtain

$$\langle (\dot{y}_2(t) - \dot{y}_1(t))(\dot{y}_2(t') - \dot{y}_1(t')) \rangle = \frac{4k_B T}{\zeta}\delta(t-t'). \quad (8)$$

From Eqs. (8), (1), and (2), the mean squared separation in the y direction grows in time according to

$$\left\langle \left[(y_2(t+\Delta t) - y_1(t+\Delta t)) - (y_2(t) - y_1(t)) \right]^2 \right\rangle = 4D_0\Delta t. \quad (9)$$

The separation in the x direction obeys the same relation. Therefore, $D^p = 2D_0$.

METHODS

We experimentally studied the dynamics of λ DNA molecules (48.5 kbp, New England Biolabs) that were fluorescently stained using YOYO-I dye at a 10: 1 base-pair-to-dye ratio. The DNA was suspended in 20 mM Tris-EDTA (TE) buffer that was titrated to pH 8.0 using HCl. 4% β-mercaptoethanol was added to suppress photobleaching. The DNA suspension was diluted to a final concentration of 0.2 μg/mL before being introduced into a nanofluidic device.

The device featured a nanoslit with height H = 110 nm, length L = 3.5 mm, and width of 160 μm (Fig. 1). Two U-shaped microchannels, each 0.55 μm deep, connected the nanoslit to two pairs of reservoirs. The nanofluidic device was fabricated in a glass chip according to methods described previously [11].

After introducing DNA into the reservoirs, a pressure-driven flow guided molecules through the microchannel on one side. A brief increase in pressure in that microchannel was applied to push the DNA molecules into the nanoslit.

V(t) was imposed as shown in Fig. 1 using Ag/AgCl electrodes immersed in reservoirs on either side of the nanoslit. A data acquisition card (DAQ, National Instruments USB-6251) generated the white Gaussian noise

signal. We used the white Gaussian noise option that is built into the signal generation module in LabVIEW control software. The software generates a series of random numbers with a variance at a sampling rate that we determine. Those random numbers drive the voltage output of the DAQ after applying a scaling factor that we adjust to control the noise level. The DAQ's maximum sampling rate of 10 kHz and maximum voltage output of 10 V placed practical limits on how close the artificial noise could come to ideal white Gaussian noise. In practice we limited the variance of the noise output from the DAQ to 2 V so that white Gaussian noise could be approximated with voltage fluctuations as large as 5 standard deviations from the mean. A voltage amplifier with a gain of 18 amplified the output from the DAQ to give $V(t)$, the voltage applied across the nanoslit. We estimate that about 80 % of the voltage applied between the reservoirs dropped across the nanoslit, based on the dimensions of the device and assuming a constant fluid conductivity.

The optical microscopy system included a 60× water immersion objective lens with a numerical aperture of 1.20 and an Andor EMCCD camera (iXon 897). Images were acquired at the rate of 2 frames per second with an exposure time of 50 ms per frame. A physical shutter was used to control the exposure time in order to reduce photo-bleaching of the stained DNA molecules. Each recording of a molecule contained 100 frames. In order to suppress possible edge effects, we only considered molecules that were at least 20 μm away from the edges of the nanoslit. 20 μm is more than 180 times the height of the nanoslit. Consequently, hydrodynamic interactions with the nanoslit edges should be completely screened [25].

Finally, custom-written image analysis software extracted the trajectories of individual molecules from the image sequences. The center-of-mass (COM) of each molecule was found by computing the first moment of its fluorescence intensity distribution. These image analysis methods have previously been described in detail [11].

RESULTS AND DISCUSSION

The addition of voltage noise significantly increased the amplitude of the Brownian motion in the y direction. Figure 2(a) shows a sequence of images of a fluorescently labeled λ DNA molecule inside a nanoslit moving under the influence of thermal forces alone. The COM of the molecule moved only about 2 μm in the x and y directions in $40s$ (although the DNA configuration changed noticeably in that time).

Figure 2(b) shows a similar sequence of images, except in this case diffusion was assisted by an applied voltage noise with $\sigma_e = 36V$. The COM moved about 15 μm in the y direction and about 2 μm in the x direction in $40s$.

Figure 2(c) compares the trajectories of a selection of DNA molecules moving with and without added $\sigma_e = 36V$ electrical noise, clearly showing that the added electrical noise amplified the fluctuations.

Figure 2(d) compares the dependence of MSD on Δt for molecules experiencing only thermal noise with the dependence for molecules subjected to a noise level of $\sigma_e = 36V$. We obtained D_x and D_y by fitting Eq. 1 to the slopes of the data. In the case of pure thermal diffusion ($\sigma_e = 0$), the diffusion coefficients were $D_x = 0.130 \pm 0.006$ $\mu\mathrm{m}^2\mathrm{s}^{-1}$ in the x direction and $D_y = 0.137 \pm 0.005$ $\mu\mathrm{m}^2\mathrm{s}^{-1}$ in the y direction. With the addition of $\sigma_e = 36V$ noise, the diffusion coefficient in the y direction increased by a factor of approximately 19 (to $D_y = 2.5 \pm 0.3$ $\mu\mathrm{m}^2\mathrm{s}^{-1}$), but the diffusion coefficient in the x direction ($D_x = 0.21 \pm 0.07$ $\mu\mathrm{m}^2\mathrm{s}^{-1}$) was not significantly altered.

We measured the dependence of D_x and D_y on the electrical noise level by analyzing the growth in MSD with time. We studied 50-70 DNA molecules for each of the 8 different values of σ_e tested. Figure 3 shows the dependence of the mean D on σ_e^2 for both the x and y directions. D_y increased linearly with σ_e^2, while D_x was relatively insensitive to σ_e.

Based on Eq. (6), we fit the function $D = D_0 + \alpha\sigma_e^2$ to the measured data in Fig. 3, using D_0 and α as fitting parameters. In the x direction the fit obtained $D_{0,x} = 0.130 \pm 0.003$ $\mu\mathrm{m}^2\mathrm{s}^{-1}$ and $\alpha_x = (0.014 \pm 0.007) \times 10^{-3}$ $\mu\mathrm{m}^2\mathrm{s}^{-1}\mathrm{V}^{-2}$; the small increase of D_x with noise level is not predicted by Eq. (4), but could have been caused either by inhomogeneities in the channel that give rise to lateral (x direction) electric field components or a slight misalignment of the fluidic channel relative to rows and columns of camera pixels. In the y direction the fit obtained $D_{0,y} = 0.139 \pm 0.005$ $\mu\mathrm{m}^2\mathrm{s}^{-1}$ and $\alpha = 1.82 \pm 0.06 \times 10^{-3}$ $\mu\mathrm{m}^2\mathrm{s}^{-1}\mathrm{V}^{-2}$. The values of $D_{0,y}$ and D_0, which were measured independently, are the same within experimental error; this was predicted by Eq. 6. The measured value of α enables us, through $\alpha = \mu^2/(4BL^2)$ from Eq. 6, to find the DNA mobility inside the nanoslit: We found $\mu = (2.11 \pm 0.16) \times 10^4$ $\mu\mathrm{m}^2\mathrm{s}^{-1}\mathrm{V}^{-1}$. That value includes contributions from DNA's electrophoresis through the fluid and the electroosmotic flow of fluid within the channel. We note that it is similar in magnitude to the free electrophoretic mobility of double-stranded DNA in Tris-borate-EDTA buffer, 4.5×10^4 $\mu\mathrm{m}^2\mathrm{s}^{-1}\mathrm{V}^{-1}$ [26].

The enhancement of DNA fluctuations in the y direction can be interpreted as an increase in the effective temperature caused by $V(t)$. We calculated T_{eff} using Eq. (7), with $T_0 = 298 \pm 2$ K being the true thermal temperature. T_{eff} increased linearly with σ_e^2 and reached a maximum of 5,300 K at the highest noise level, $\sigma_e = 36$ V (Fig.3).

We investigated the spatial correlations of electrokinetic noise by measuring the relative displacements of pairs of DNA molecules subjected to the same $V(t)$ with

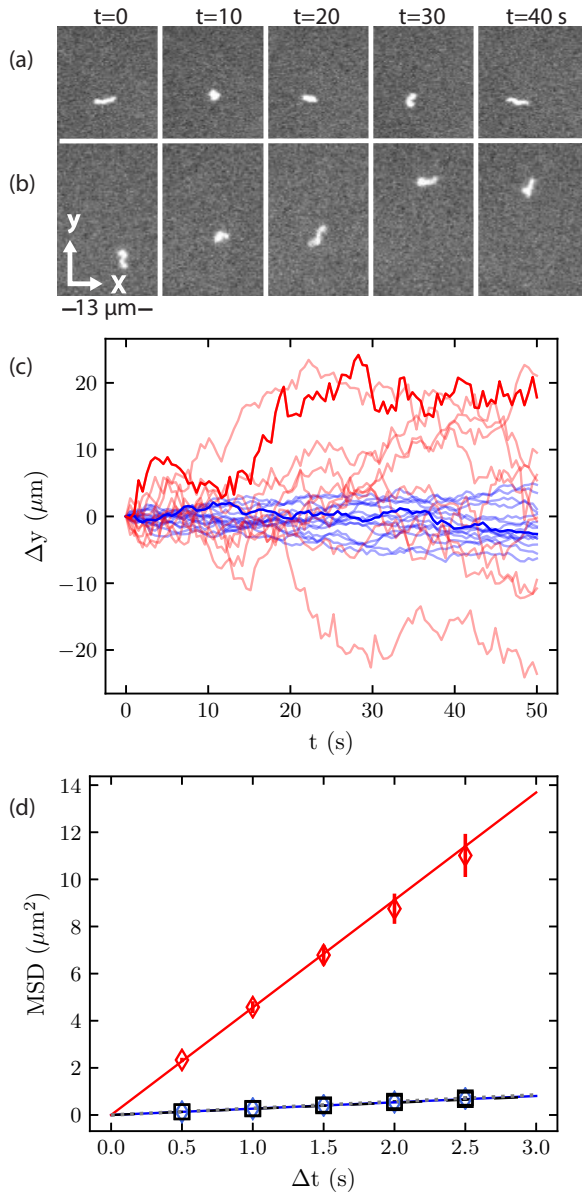

FIG. 2. (a) Time-resliced images of a fluorescently labeled λ DNA molecule diffusing in TE buffer with no voltage noise and (b) with a voltage noise level of $\sigma_e = 36V$. (c) λ DNA trajectories in the y direction with no applied noise (blue) and an applied noise level of $\sigma_e = 36V$ (red). The two bold lines correspond to the molecules shown in (a) and (b). (d) Dependence of the MSD on Δt, with diamonds indicating the y direction and squares the x direction. Blue symbols indicate no applied noise and red symbols a noise level of $\sigma_e = 36V$. Lines are linear fits to the data. The lines for y-motion with no added noise (solid), x-motion with no added noise (dotted), and x motion with $\sigma_e = 36V$ (dashed) all overlap. All measurements were performed in the same $H = 110nm$ slit. Error bars represent one standard deviation.

$\sigma_e = 18$ V. Figure 4 plots the growth in the mean square distance between the centers of mass, in both the x and

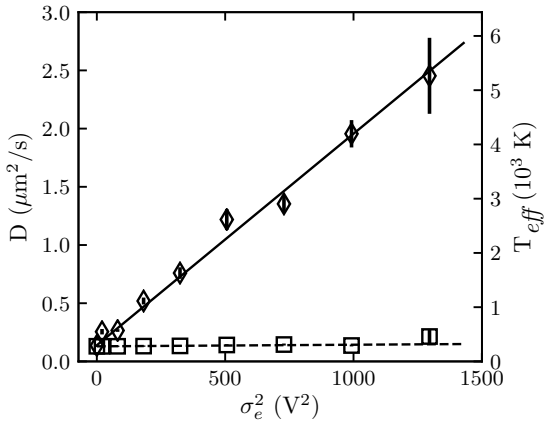

FIG. 3. Dependence of D on σ_e in the x (squares) and y (diamonds) directions. Lines are linear fits using $D = D_0 + \alpha\sigma_e^2$. Right axis indicates the corresponding effective temperature. Error bars are the standard error from a bootstrap analysis of 1000 re-samplings of diffusion coefficients of DNA molecules.

y directions, for 20 such pairs. The MSD for the pairs increased linearly with time, with very similar slopes for the x and y directions. The slopes reflect pairwise diffusion coefficients, D^p. Using Eq. 1, we found $D_x^p = 0.25 \pm 0.01$ μm^{2}s^{-1} and $D_y^p = 0.26 \pm 0.01 \mu m^2 s^{-1}$ in the x and y directions, respectively. Those values are almost exactly double the thermal diffusion coefficient of a single molecule in one dimension, $D_0 = (0.13 \pm 0.01)$ μm^{2}s^{-1}, which we obtained from the trajectories of the same molecules analyzed individually.

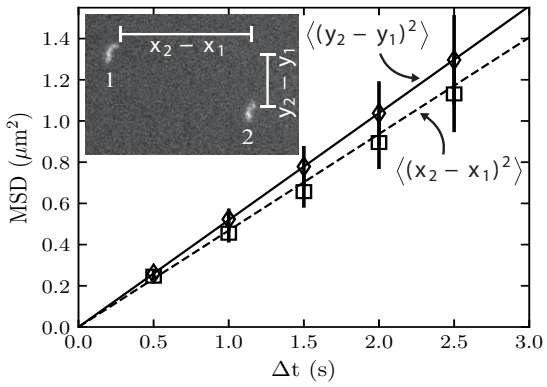

FIG. 4. The mean-squared separation between two λ DNA molecules subjected to the same $\sigma_e = 18$ V voltage noise is plotted as a function of time for the x (squares) and y (diamonds) directions. Lines are linear fits to the x (dashed) and y (solid) data.

The spatially correlated nature of electrokinetic forces explains why a double-stranded DNA molecule can survive much higher effective temperatures than thermal

temperatures. No tension, compression, or shear builds up in the molecule as the result of electrokinetic noise. Thermal forces, on the other hand, are applied in random directions to different parts of a molecule. The resulting stresses must be balanced by internal molecular binding forces, and a molecule loses its ability to do that above the melting temperature.

Figure 5 shows the dependence of the DNA radius of gyration, R_g, on σ_e. R_g was obtained from analyses of the molecular fluorescence intensity distributions, as described in Ref. [27]. R_g was relatively insensitive to σ_e: The mean value was 1.04 ± 0.01 μm, and a linear fit found that R_g increased by only 5% of its initial value over the full range of σ_e. These observations lead us to conclude that the observed changes in diffusivity with σ_e are not caused by changes in the hydrodynamic radius of the DNA.

The technique described here opens up new possibilities for studying noise-driven phenomena in nanofluidic devices. For example, Kramers' kinetics can be studied in a new regime. The starting point for Kramers' theoretical model of reaction rates is a Langevin equation with an energy landscape featuring a barrier and a white Gaussian noise term whose delta-correlated amplitude characterizes the temperature [1]. The same model describes the dynamics of DNA in our experiments, except the noise term in Eq. 5 combines electrokinetic and thermal forces, which are uncorrelated but have the same statistical properties. Thus, like Kramers' model, Eq. 5 obtains the familiar Arrhenius kinetics, but with an effective temperature defined by Eq. 7. It is also straightforward to create free energy barriers for DNA in nanofluidic devices by defining pits and constrictions, which respectively increase or decrease the configuration entropy of a confined polymer [27–29]. In a nanoslit with an embedded nanotopography, long DNA molecules become trapped inside nanopits where their configuration entropy is relatively high, and to hop to a neighboring pit, the molecule must overcome an entropic barrier in the free energy landscape [27, 29, 30]. Raising T does not significantly increase the hopping rate in this system because the entropic barrier, which results from thermal fluctuations of segments within a molecule, also grows in proportion with T. But our electrokinetic technique grants us control over the fluctuations in a polymer's center of mass independently of the thermal fluctuations of its segments. Raising T_{eff} should leave the entropic barrier unchanged and enable us to manipulate the hopping rate over a wide and interesting range.

Stochastic resonance (SR) is another noise-assisted phenomenon one could study in new ways with electrokinetic noise. SR involves a nonlinear system whose response to a weak periodic signal obtains a maximum for some optimum noise level [12, 13, 31]. In a nanofluidic experiment involving DNA, the hallmark of SR would be a maximum in the synchronization between a weak periodic driving force and the hopping of a DNA molecule back and forth between two nanopits as a function of T_{eff}. To observe that in practice, one needs to vary the noise level over an extremely wide range and independently of the barriers between pits. An ability to raise T_{eff} to otherwise impossible levels also raises the possibility of studying nonequilibrium dynamical phenomena, which have attracted growing interest recently [11, 32–36].

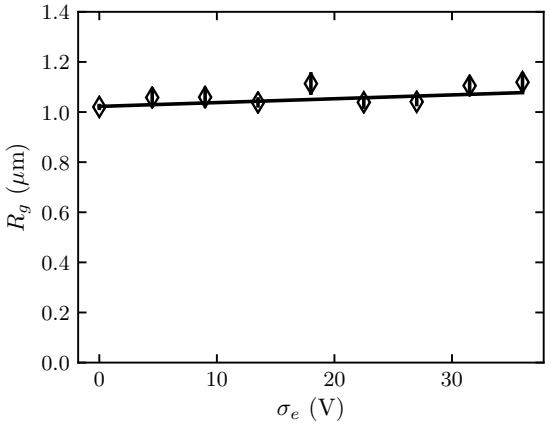

FIG. 5. Dependence of R_g on σ_e. Each point is the mean R_g of the λ DNA molecules measured for each σ_e; the same molecules were analyzed in Fig. 3. The line is a linear fit.

CONCLUSION

In conclusion, electrokinetic noise offers a convenient means of controlling and amplifying the Brownian motion of DNA molecules in nanofluidic devices. The technique can achieve effective noise temperatures well above the DNA melting point without compromising its structural integrity or affecting the thermal fluctuations that determine its configuration entropy. These features make electrokinetic noise an appealing lever of control for investigating noise-driven nanofluidic phenomena.

This material is based upon work supported by the National Science Foundation under Grants No. 1409577 and No. 1904511.

* derek_stein@brown.edu

[1] Peter Hänggi, Peter Talkner, and Michal Borkovec. Reaction-rate theory: fifty years after kramers. *Reviews of modern physics*, 62(2):251, 1990.

[2] TN Palmer. Stochastic weather and climate models. *Nature Reviews Physics*, 1(7):463–471, 2019.

[3] Gregor Neuert, Brian Munsky, Rui Zhen Tan, Leonid Teytelman, Mustafa Khammash, and Alexander van Oudenaarden. Systematic identification of signal-activated stochastic gene regulation. *Science*, 339(6119):584–587, 2013.

[4] Fischer Black. Noise. *The journal of finance*, 41(3):528–543, 1986.

[5] Albert Einstein. On the motion of small particles suspended in liquids at rest required by the molecular-kinetic theory of heat. *Annalen der physik*, 17:549–560, 1905.

[6] George E Uhlenbeck and Leonard S Ornstein. On the theory of the brownian motion. *Physical review*, 36(5):823, 1930.

[7] John F Brady. Brownian motion, hydrodynamics, and the osmotic pressure. *The Journal of chemical physics*, 98(4):3335–3341, 1993.

[8] C Bustamante, JF Marko, ED Siggia, and S Smith. Entropic elasticity of λ-phage DNA. *Proc. Nati. Acad. Sci USA*, 88:10009, 1991.

[9] Sho Asakura and Fumio Oosawa. On interaction between two bodies immersed in a solution of macromolecules. *The Journal of chemical physics*, 22(7):1255–1256, 1954.

[10] Daniel Rudhardt, Clemens Bechinger, and Paul Leiderer. Direct measurement of depletion potentials in mixtures of colloids and nonionic polymers. *Physical review letters*, 81(6):1330, 1998.

[11] Daniel Kim, Clark Bowman, Jackson T. Del Bonis-O'Donnell, Anastasios Matzavinos, and Derek Stein. Giant acceleration of DNA diffusion in an array of entropic barriers. *Phys. Rev. Lett.*, 118:048002, Jan 2017.

[12] Peter Hänggi. Stochastic resonance in biology: How noise can enhance detection of weak signals and help improve biological information processing. *ChemPhysChem*, 3(3):285–290, 2002.

[13] Yee Joon Kim, Marcia Grabowecky, and Satoru Suzuki. Stochastic resonance in binocular rivalry. *Vision Research*, 46(3):392–406, 2006.

[14] Mesfin Asfaw and Wokyung Sung. Stochastic resonance of a flexible chain crossing over a barrier. *EPL (Europhysics Letters)*, 90(3):30008, 2010.

[15] Peter Hänggi. Escape over fluctuating barriers driven by colored noise. *Chemical physics*, 180(2-3):157–166, 1994.

[16] Yong Woon Kim and Wokyung Sung. Does stochastic resonance occur in periodic potentials? *Physical Review E*, 57(6):R6237, 1998.

[17] Adam E Cohen and WE Moerner. Method for trapping and manipulating nanoscale objects in solution. *Applied physics letters*, 86(9):093109, 2005.

[18] CKS Miller, WC Daywitt, and MG Arthur. Noise standards, measurements, and receiver noise definitions. *Proceedings of the IEEE*, 55(6):865–877, 1967.

[19] Grzegorz Szamel. Self-propelled particle in an external potential: Existence of an effective temperature. *Physical Review E*, 90(1):012111, 2014.

[20] Luca Gammaitoni, Peter Hanggi, Peter Jung, and Fabio Marchesoni. Stochastic resonance. *Reviews of modern physics*, 70(1):223, 1998.

[21] Masao Doi. *Soft matter physics*. Oxford University Press, 2013.

[22] Sushanta Dattagupta. *Diffusion: Formalism and Applications*. CRC Press, 2013.

[23] Thomas M Cover and Joy A Thomas. *Elements of information theory*. John Wiley & Sons, 2012.

[24] Rik Pintelon, Johan Schoukens, and Patrick Guillaume. Continuous-time noise modeling from sampled data. *IEEE Transactions on Instrumentation and Measurement*, 55(6):2253–2258, 2006.

[25] Kevin D Dorfman, Damini Gupta, Aashish Jain, Abhiram Muralidhar, and Douglas R Tree. Hydrodynamics of dna confined in nanoslits and nanochannels. *The European Physical Journal Special Topics*, 223(14):3179–3200, 2014.

[26] Nancy C Stellwagen, Cecilia Gelfi, and Pier Giorgio Righetti. The free solution mobility of DNA. *Biopolymers: Original Research on Biomolecules*, 42(6):687–703, 1997.

[27] JT Del Bonis-O'Donnell, Walter Reisner, and Derek Stein. Pressure-driven DNA transport across an artificial nanotopography. *New Journal of Physics*, 11(7):075032, 2009.

[28] Jongyoon Han and Harold G Craighead. Separation of long DNA molecules in a microfabricated entropic trap array. *Science*, 288(5468):1026–1029, 2000.

[29] Walter Reisner, Niels B Larsen, Henrik Flyvbjerg, Jonas O Tegenfeldt, and Anders Kristensen. Directed self-organization of single DNA molecules in a nanoslit via embedded nanopit arrays. *Proceedings of the National Academy of Sciences*, 106(1):79–84, 2009.

[30] Elijah Shelton, Zhijun Jiang, Shutong Wang, and Derek Stein. Controlling the conformations and transport of dna by free energy landscaping. *Applied Physics Letters*, 99(26):263112, 2011.

[31] Roberto Benzi, Giorgio Parisi, Alfonso Sutera, and Angelo Vulpiani. Stochastic resonance in climatic change. *Tellus*, 34(1):10–16, 1982.

[32] Christopher Battle, Chase P Broedersz, Nikta Fakhri, Veikko F Geyer, Jonathon Howard, Christoph F Schmidt, and Fred C MacKintosh. Broken detailed balance at mesoscopic scales in active biological systems. *Science*, 352(6285):604–607, 2016.

[33] Jakub Spiechowicz, Marcin Kostur, and Jerzy Łuczka. Brownian ratchets: How stronger thermal noise can reduce diffusion. *Chaos: An Interdisciplinary Journal of Nonlinear Science*, 27(2):023111, 2017.

[34] Yizhou Tan, Jannes Gladrow, Ulrich F Keyser, Leonardo Dagdug, and Stefano Pagliara. Particle transport across a channel via an oscillating potential. *Physical Review E*, 96(5):052401, 2017.

[35] Alexander R Klotz, Beatrice W Soh, and Patrick S Doyle. Motion of knots in dna stretched by elongational fields. *Physical review letters*, 120(18):188003, 2018.

[36] Angus McMullen, Hendrick W de Haan, Jay X Tang, and Derek Stein. Buckling causes nonlinear dynamics of filamentous viruses driven through nanopores. *Physical review letters*, 120(7):078101, 2018.